

58702  
17426

**Analysis of a High-Lift Multi-Element Airfoil  
Using a Navier-Stokes Code**

1995 LARSS Program Participant:  
Mark E. Whitlock

Mentor:  
Kenneth M. Jones

NASA Langley Research Center  
Research and Technology Group  
Aerodynamics Division  
Subsonic Aerodynamics Branch

## ABSTRACT

A thin-layer Navier-Stokes code, CFL3D, was utilized to compute the flow over a high-lift multi-element airfoil. This study was conducted to improve the prediction of high-lift flowfields using various turbulence models and improved gridding techniques. An overset Chimera grid system is used to model the three element airfoil geometry. The effects of wind tunnel wall modeling, changes to the grid density and distribution, and embedded grids are discussed. Computed pressure and lift coefficients using Spalart-Allmaras, Baldwin-Barth, and Menter's  $\kappa\text{-}\omega$  SST turbulence models are compared with experimental data. The ability of CFL3D to predict the effects on lift coefficient due to changes in Reynolds number changes is also discussed.

## INTRODUCTION

Improving the cruise and high-lift efficiency of commercial subsonic transports has received increased attention in recent years. Current wing designs produce higher cruise lift coefficients than those of years past. The higher lift coefficients reduce the wing area required at cruise conditions. At the present time however, takeoff and landing requirements dictate the wing area of a commercial aircraft. This is in part due to inefficiencies in the high-lift systems. More efficient high-lift system designs will allow trade studies to be performed to improve the overall aircraft system. One such tradeoff is to reduce the size of the wing (and possibly reduce the cost of the aircraft).

Researchers are currently investigating ways to use computational fluid dynamics (CFD) to improve the aerodynamic performance of three dimensional (3D) high-lift systems. This task is very complicated, largely due to complex flow physics and grid generation issues. Many of the issues in 3D grid generation also exist in 2D. The time required to create a 2D grid and perform multiple analyses, however, is much less than that for a 3D grid. Many researchers, therefore, are studying 2D geometries to gain insight into the complex fluid physics of high-lift flowfields that will in turn help the understanding of 3D high-lift systems.

The geometry used for this study is a three element airfoil (slat, main element, and flap) that was designed by Douglas Aircraft. The geometry was sent to several universities, aerospace corporations, and NASA centers as part of the NASA High-Lift CFD Challenge Workshop in 1993. The purpose of the CFD Challenge was to define the state-of-the-art in 2D multi-element airfoil prediction codes. This optimized airfoil and its extensive experimental aerodynamic database is currently being used throughout the aerospace industry as a means of calibrating CFD codes. The experimental database includes forces, skin friction distributions, and velocity and total pressure profiles for two geometries at Reynolds numbers of 5 and 9 million. The task assigned for the summer was to investigate methods to improve the correlation between the experimental data and computational results. These methods include wind tunnel wall modeling, selection of turbulence models, and improving the grids which define the airfoil geometry.

## APPROACH

Several key issues were investigated in an attempt to more accurately predict the flow over the Douglas airfoil. Building on the work of Ken Jones and others at the CFD Challenge, three key issues were investigated to improve the flow solution for the Douglas airfoil. Research conducted by H.V. Cao<sup>1</sup>, et al., of the Boeing Company indicates that the wind tunnel walls have to be modeled in order to make an accurate comparison between the computational results and the experimental data. One task for the summer was improve the wind tunnel wall modeling and to correct the implementation of the tunnel boundary conditions. A second task for the summer was to improve on the existing grid that was used during last summer's analysis. This study investigated improvements in the Chimera grid cutouts, embedded grids, and the effect of grid density on the flow solution. A third task was to investigate the effects of turbulence models on the flow solution. The Spalart-Allmaras, Baldwin-Barth, and Menter's  $\kappa$ - $\omega$  SST turbulence models were used for this investigation. Finally, CFL3D's ability to predict changes in lift coefficient due to Reynolds number changes was investigated.

The high-lift geometry was modeled using a gridding technique known as overlapped or Chimera gridding. For the Chimera gridding scheme, the overlapped grids are each created independently. MAGGIE cuts holes in the individual grids along user defined boundaries so that no grids overlap the airfoil surfaces. The final grids used for this analysis are shown in Figure 1 (for clarity only every other grid point is shown). A total of six grids were used: a tunnel grid, main element grid, slat grid, flap grid, flap trailing edge grid, and cove grid. MAGGIE then creates interpolation stencils which the flow solver, CFL3D, uses to pass information between grids. One benefit of the Chimera gridding is that the individual grid blocks are created

independently, so a change in flap location or rotation for example will not effect the design of the individual grid blocks. It will only effect the hole cutout and interpolation stencils. These grids are then analyzed using the Reynolds-averaged Navier-Stokes code, CFL3D. CFL3D solves the 3D, compressible Navier-Stokes equations using thin-layer approximations. To accelerate convergence, the code uses multi-gridding and local time-stepping techniques.

The approach used for this research involved first determining what improvements could be made in the flow solutions in light of work presented at the 13th AIAA Applied Aerodynamics Conference.<sup>2</sup> The procedure used involved first making modifications to the grids used or flow solver input files, and then running these grids through the flow solver CFL3D. Unless otherwise specified, all runs in this study were computed at the following conditions:  $\alpha = 16.02^\circ$ ,  $Re = 9 \times 10^6$ ,  $M_\infty = 0.2$ . Also, unless stated otherwise, all solutions were obtained using the Spalart-Allmaras turbulence model. Only one change was made to the grids at a time. This allowed the results to be compared to past solutions and determine what the effect of each change was. This approach allowed a better understanding of the effects of different grids and of the fluid physics around the airfoil.

## LANGLEY RESEARCH CENTER EQUIPMENT AND FACILITIES USED

This project required the use of several computer systems at Langley. Grid generation and post-processing was done on a Silicon Graphics IRIS 4D25 workstation. Complex calculations, including running the flow solver and grid adaptation, were performed on Sabre, a Cray YMP located at the NASA Langley Research Center. Storage of the input files and flow solutions were made possible through the Mass Storage Subsystem on Sabre. All experimental results were provided by a wind tunnel test conducted in Langley's Low Turbulence Pressure Tunnel (LTPT).

## RESULTS

### Wind Tunnel Walls

It is believed that the wind tunnel wall corrections currently used in the LTPT may become inaccurate at high lift coefficients, particularly near maximum lift. Therefore, the best way to calibrate a code with this dataset is to use experimental data which has not been corrected for wall interference or tunnel blockage effects and model the wind tunnel walls. Care must be taken when modeling the wind tunnel, however, to properly set the tunnel boundary conditions to those used in the LTPT. Two changes were made to the tunnel modeling from last summer. First, the tunnel inlet plane was extended further upstream. And second, the tunnel back pressure was adjusted to more accurately match LTPT reference conditions.

The first change made on last summer's tunnel grid was to extend the inlet plane further upstream. The inlet from last summer's grid was approximately four chords upstream of the model leading edge<sup>1</sup>. Cao demonstrated that the inlet for the tunnel is best if extended at least five chords upstream of the leading edge. If the inlet is closer to the leading edge, the constant Mach number boundary conditions set on the inlet plane will over-constrain the solution. To correct this problem, two grid changes were made. The first extended the tunnel out to six chords upstream of the leading edge (Figure 1d), and the second to eight chords. It was found that by extending the inlet to six chords dropped the lift coefficient by approximately 0.013. Extending the inlet to eight chords produced only negligible changes in the lift coefficient. This seems to confirm Cao's results and indicates that the tunnel inlet should be at least five chords upstream of the model leading edge for accurate computations. The remainder of this study was completed with the six chord tunnel grid.

The second change made in modeling the wind tunnel was a change in the tunnel exit boundary condition. Last summer the back pressure was computed using the isentropic flow equations and assuming an isentropic expansion through the diffuser. It was found, however, that this is not the method used to set the LTPT reference conditions. The LTPT flow conditions are set using static and total pressures at tunnel station -64.0 (which is approximately 53 inches upstream of the slat). The tunnel conditions are adjusted until the pressures at this tunnel station match those from an empty tunnel calibration. It was found that the back pressure calculated from the isentropic expansion did not yield pressures at station -64.0 which match the calibration curve. Thus, the tunnel back pressure was increased until the static and dynamic pressures matched the reference conditions used for the LTPT data. It is still unclear why the back pressure calculated by the isentropic expansion formulas did not match the back pressure required to match the reference conditions at station -64.0. Using the correct back-pressure, however, resulted in a decrease in the lift coefficient of nearly 0.03.

### Grid Improvements

The second task was to make improvements to the grids used to model the multi-element airfoil geometry. Five studies were completed in an attempt to more accurately match the experimental data. The first study resulted in an improved flap grid. Second, the main element and cove grids were modified to better resolve the flow over the flap. A grid resolution study was performed on this new grid. Finally, an embedded grid was used in an attempt to better resolve the off-body flowfield above the flap.

The first improvement made to the grid from last summer was on the flap grid. The flap grid used last summer extended approximately one flap chord in all directions from the flap surface.<sup>2</sup> The grid spacing near the flap grid boundary was very sparse. Not only were the sparse grid points far from the surface of the grid a waste of points, but the grid may have added a form of dissipation to the flap flowfield. To remedy the situation, the flap grid was cut to approximately 0.2 flap chords from the surface of the flap (Figure 1b). Cutting the outer boundary of the flap grid resulted in a negligible change in forces or pressure distributions on the airfoil.

The second major change made to the grid was to add more grid points above the flap on the main element and cove grids. Work by Rogers<sup>3</sup> demonstrated how very complex the flowfield above the flap can be, especially at high angles of attack. There was concern that the grid used last summer was too sparse in the streamwise direction on the main element to resolve this complex flowfield. To remedy this situation, approximately twenty points were added in the streamwise direction to the main element grid. Due to temporary problems with the patching routines in CFL3D, the cove grid had to have an equal number of points added in the streamwise direction to maintain a one-to-one matching along the grid boundary. Adding these points to the main element and cove grids increased the time required to obtain a converged solution. More importantly, however, a comparison of surface pressures demonstrated that the new grids improved the ability of the code to capture the flow physics.

In an attempt to decrease the time required to generate a flow solution, a normal direction grid resolution study was performed on the main element and slat. Last summer the main element and slat grids were doubled in points in the normal direction to better resolve the slat wake over the main element. It was believed that after a solution adaptation was done to the main element grid in the slat region this grid doubling became unnecessary. Thus, to increase convergence rates the main element was reduced from 161 points in the normal direction to 117 points. The points were removed from near the surface of the airfoil while maintaining  $y^+$  values of less than 1.0. Removing these points resulted in only minimal change to the flow solution. Similarly, every other point in the normal direction of the slat was removed, reducing the size of the slat grid from 145 to 73 normal points with an even smaller change in the flow solution. By reducing the grid sizes in the normal direction about 30,000 grid points were removed resulting in decreased computer resource requirements with minimal changes in the flow solution. A plot of the pressure distributions over the airfoil is shown in Figure 2. Note that there is excellent agreement between

the experimental and computational pressure profiles over the main element and slat. The flap, however, shows a leveling off of the pressure profile indicative of separation which the experimental data does not support. It is not known whether this separation on the flap is due to the grids or turbulence model.

The experimental flowfield data for the Douglas airfoil indicates that near the maximum lift coefficient there is a region of off-body separation above the flap.<sup>4</sup> The new main element grid greatly improved the ability of CFL3D to resolve this flowfield but as shown in Figure 2, the flap pressures do not closely match the experimental values. An embedded grid was placed above the flap to try and correct the flap pressure distributions. For the 16° and 21° angle of attack cases the embedded grid made very minor changes to the pressure distributions over the airfoils. A successful solution was not obtained with the embedded grid on the airfoil at 8° angle of attack.

### Turbulence Models

High-lift, multi-element flowfields are dominated by viscous phenomenon. Computational studies have shown that the choice of turbulence model can have a large effect on pressure contours, velocity profiles, and overall forces. Studies completed by Rogers<sup>3,5</sup> and others have shown the Baldwin-Barth (BB) and Menter's  $\kappa$ - $\omega$  SST (SST) turbulence models often are more accurate at modeling the turbulence found in high-lift flowfields than the Spalart-Allmaras (SA) turbulence model. To determine the effect of turbulence models on lift coefficient a turbulence model study was performed using the SA, BB, and SST turbulence models at Reynolds numbers of 5 and 9 million. Figure 3 shows the lift coefficient versus angle of attack for the three turbulence models at these Reynolds numbers. Note that the Spalart-Allmaras turbulence model yields a lift coefficient which is significantly higher than the experimental values at all angles of attack. The Baldwin-Barth and SST turbulence models produces lift coefficients which agree very well with experimental values at 16° and 21° angle of attack. The BB and SST models, however, do not agree well with experimental values at 8° angle of attack. One possible explanation for this can lie in the fact that the experimental data shows the trailing edge of the flap to be separated at 8° angle of attack. If the grid or the turbulence model do not allow separation to be accurately predicted, then this could result in the overpredicted lift values. This has not yet been looked at and should be investigated further.

### Reynolds Number Effects

One goal of the CFD Challenge was to be able to predict changes in lift coefficient due to changes in Reynolds number. The experimental database contained results at Reynolds numbers of 5 and 9 million<sup>4</sup>. Figure 4 shows the increment in lift coefficient caused by changing from a Reynolds number of 5 million to a Reynolds number of 9 million. Note that CFL3D matches the data fairly well at 8° and 16° angle of attack, but not at 21° angle of attack. At 21° angle of attack, the experimental data suggest that there is off-body separation above the flap. This separation is stronger at a Reynolds number of 5 million. One possible cause of the poor Reynolds number predictive capability at 21° then could be that the grids or solver do not allow the off-body separation to be modeled accurately. This should be investigated further to improve the predictive capability of CFL3D.

### CONCLUSIONS

A computational study was performed to improve the predictive capability of a Navier-Stokes code for high-lift flowfields. It was determined that the wind tunnel wall should extend at least

five chords upstream of the model for accurate computations. Furthermore, the exit back pressure must be set to match the tunnel reference conditions at station -64.0, as is done in the LTPT. As shown in this study, for situations where standard wind tunnel wall corrections are inaccurate, it is important to correctly model the wind tunnel walls when analyzing the configuration.

Several improvements were made to the gridding system. The flap grid outer boundary was moved closer to the flap surface. Additional points were added in the streamwise direction to the main element above the flap and improved the ability to capture the complex flow physics. The main element and slat grids were reduced in points in the normal direction. This decreased the required computer resources with little effect on the flow solution. An embedded grid was added above the flap but produced little change in the surface pressures.

The choice of turbulence model was also found to have a large effect on the final flow solution. This study indicated that overall the Baldwin-Barth and Menter's  $\kappa\text{-}\omega$  SST turbulence models are more accurate than Spalart-Allmaras for the high-lift flowfield investigated. CFL3D was able to closely predict the effect of a change in Reynolds number on lift coefficient at low angles of attack. Near maximum lift, this predictive capability diminished.

## REFERENCES

- [1] Cao, H.V., Kusunose, K., Spalart, P.R., Ishimitsu, K.K., Rogers, S.E., McGhee, R.J., "Study of Wind Tunnel Wall Interference for Multi-Element Airfoils Using a Navier-Stokes Code", AIAA-94-1993, 1994.
- [2] Jones, K.M., Biedron, R.T., Whitlock, M.E., "Application of a Navier-Stokes Solver to the Analysis of Multielement Airfoils and Wings Using Multizonal Grid Techniques", AIAA 95-1855, 1995.
- [3] Rogers, S.E., "Progress in High-Lift Aerodynamic Calculations," *Journal of Aircraft*, Vol. 31, No. 6, P1244-1251, Nov.-Dec. 1994.
- [4] Chin, V., Peters, D., Spaid, F., and McGhee, R., "Flowfield Measurements about a Multi-Element Airfoil at High Reynolds Numbers," AIAA Paper 93-3137, July, 1993.
- [5] Rogers, S.E., Menter, F.R., Durbin, P.A., Mansour, N.N., "A Comparison of Turbulence Models in Computing Multi-Element Airfoil Flows", AIAA-94-0291, 1994.

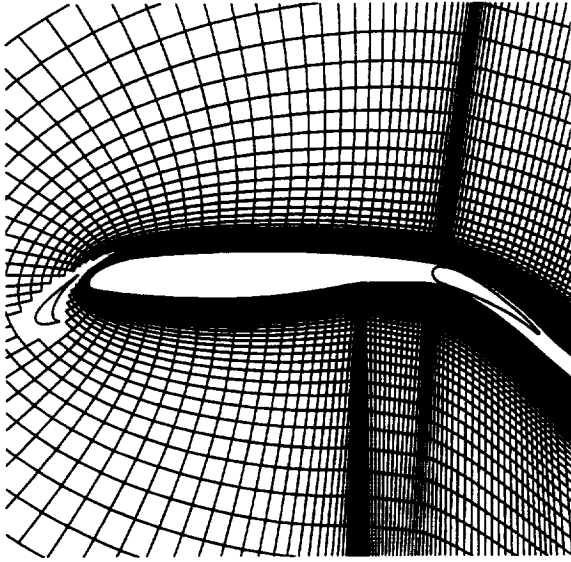


Fig. 1a. 3 element airfoil main element grid

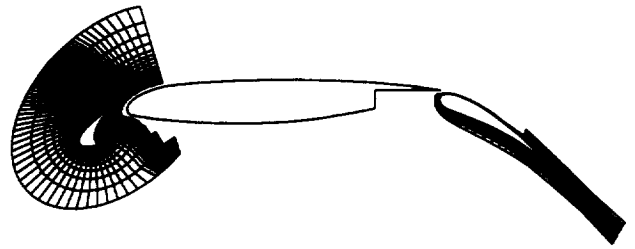


Fig. 1b. 3 element airfoil slat, flap, and flap trailing edge grids



Fig. 1c. 3 element airfoil cove grid

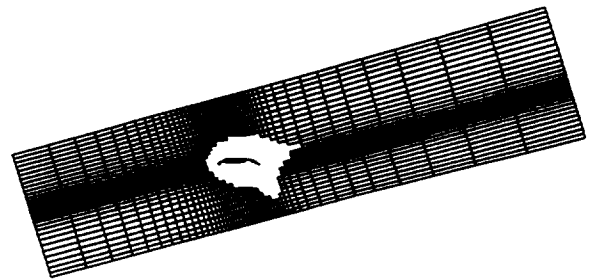


Fig. 1d. Tunnel grid

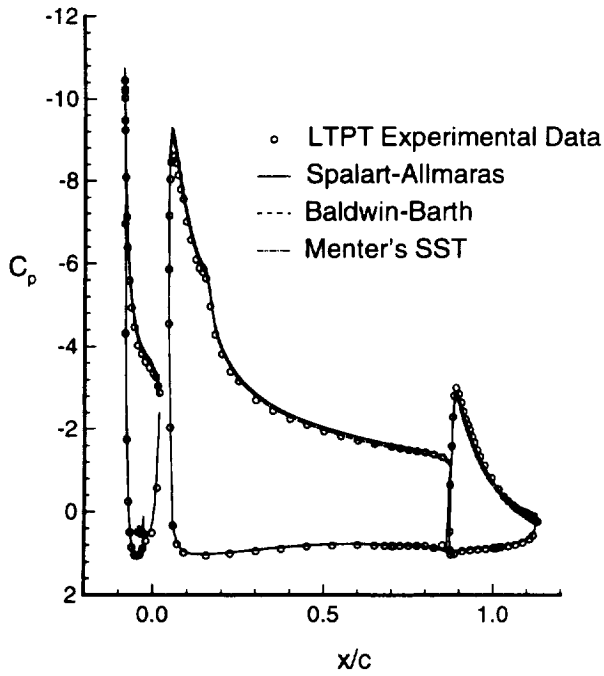


Fig. 2a. Pressure distribution,  $\alpha = 16^\circ$ ,  
 $M = 0.2$ ,  $R_e = 9 \times 10^6$

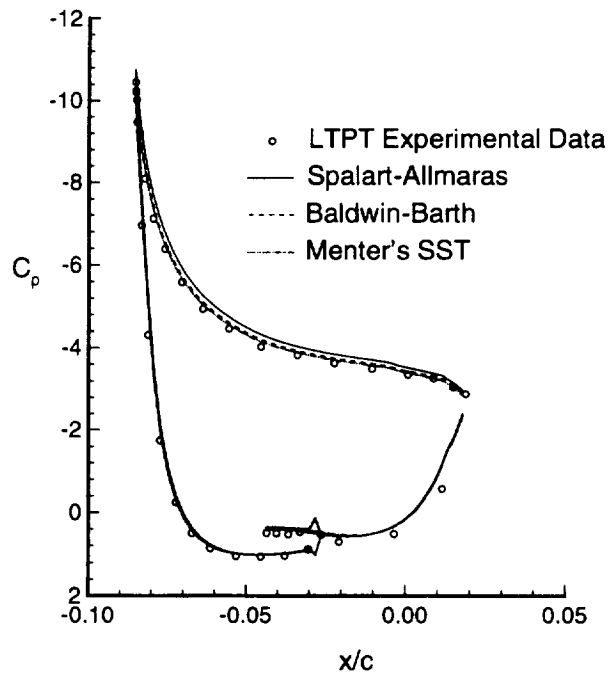


Fig. 2b. Slat pressure distribution,  $\alpha = 16^\circ$ ,  
 $M = 0.2$ ,  $R_e = 9 \times 10^6$

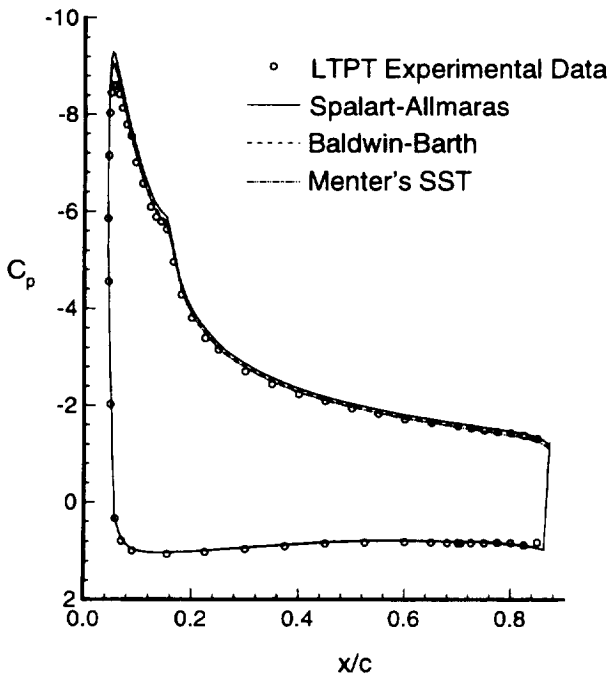


Fig. 2c. Main element pressure distribution,  
 $\alpha = 16^\circ$ ,  $M = 0.2$ ,  $R_e = 9 \times 10^6$

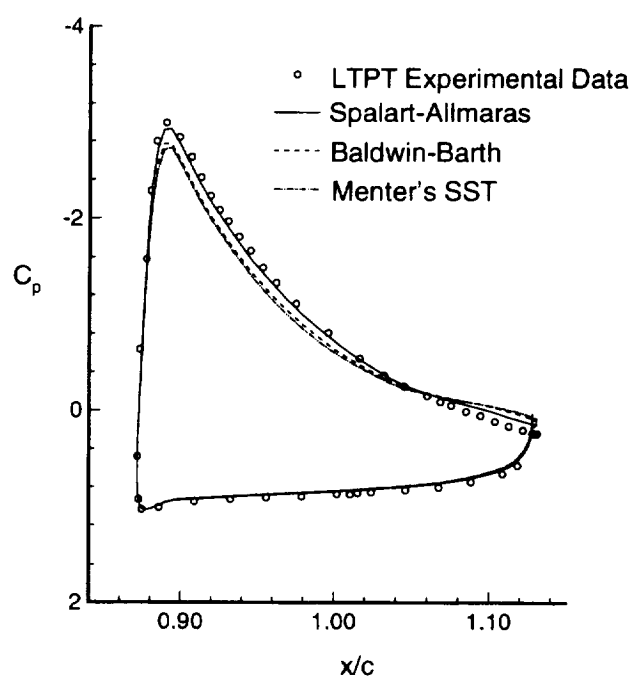


Fig. 2d. Flap pressure distribution,  $\alpha = 16^\circ$ ,  
 $M = 0.2$ ,  $R_e = 9 \times 10^6$

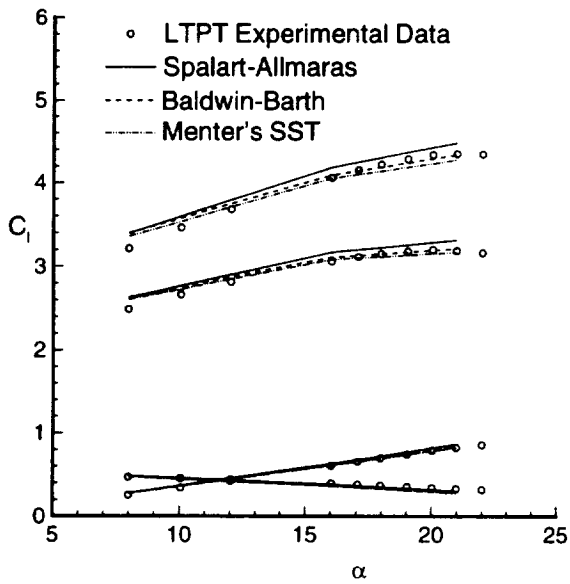


Fig. 3a. Lift curve,  $M = 0.2$ ,  $R_e = 9 \times 10^6$

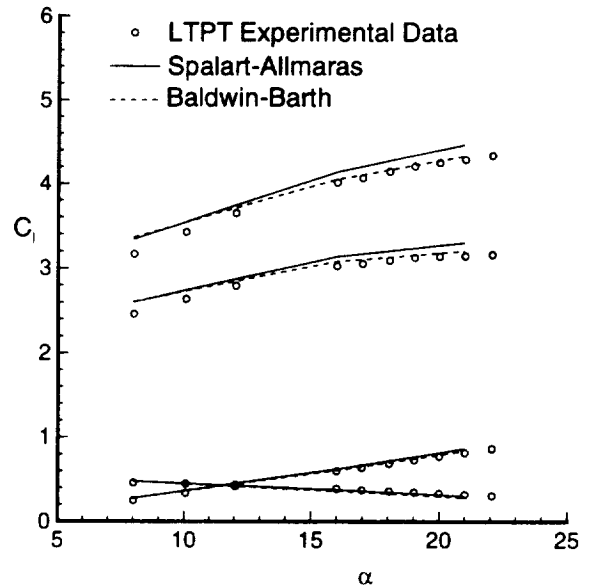


Fig. 3b. Lift curve,  $M = 0.2$ ,  $R_e = 5 \times 10^6$

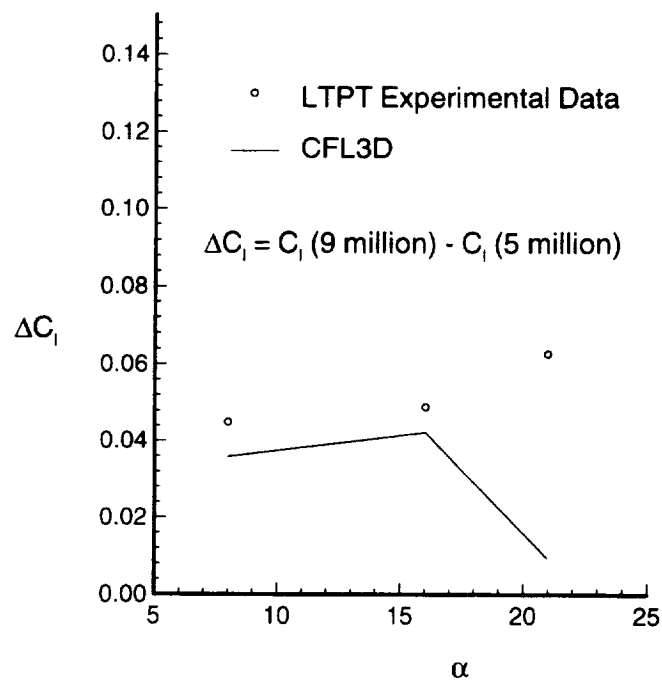


Fig. 4.  $\Delta C_l$  vs.  $\alpha$  for different Reynolds numbers